

# Laser-induced and room temperature etching of copper films by chlorine with analysis by Raman spectroscopy

Cite as: Journal of Vacuum Science & Technology A **8**, 1608 (1990); <https://doi.org/10.1116/1.576774>

Submitted: 30 August 1989 • Accepted: 18 December 1989 • Published Online: 04 June 1998

Hua Tang and Irving P. Herman



View Online




Export Citation

## ARTICLES YOU MAY BE INTERESTED IN


Nucleation and growth of CuCl thin films on commercially available SnO<sub>2</sub>/glass substrates by the sublimation method

Journal of Vacuum Science & Technology A **35**, 041511 (2017); <https://doi.org/10.1116/1.4986944>





**HIDEN**  
ANALYTICAL



40 YEARS  
1982-2022


## Instruments for Advanced Science

- Knowledge,
- Experience,
- Expertise

Click to view our product catalogue


Contact Hiden Analytical for further details:  
[www.HidenAnalytical.com](http://www.HidenAnalytical.com)  
[info@hideninc.com](mailto:info@hideninc.com)

Gas Analysis




- ▶ dynamic measurement of reaction gas streams
- ▶ catalysis and thermal analysis
- ▶ molecular beam studies
- ▶ dissolved species probes
- ▶ fermentation, environmental and ecological studies

Surface Science




- ▶ UHV-TPD
- ▶ SIMS
- ▶ end point detection in ion beam etch
- ▶ elemental imaging - surface mapping

Plasma Diagnostics



- ▶ plasma source characterization
- ▶ etch and deposition process reaction kinetic studies
- ▶ analysis of neutral and radical species

Vacuum Analysis



- ▶ partial pressure measurement and control of process gases
- ▶ reactive sputter process control
- ▶ vacuum diagnostics
- ▶ vacuum coating process monitoring

# Laser-induced and room temperature etching of copper films by chlorine with analysis by Raman spectroscopy

Hua Tang and Irving P. Herman

Department of Applied Physics and the Microelectronics Sciences Laboratories, Columbia University, New York, New York 10027

(Received 30 August 1989; accepted 18 December 1989)

The reactions of copper films on glass with chlorine are studied at room temperature with and without a focused laser (4880 Å) present for localized heating. Raman scattering is used to follow the transformation of the copper film *in situ* to the copper chlorides, CuCl and CuCl<sub>2</sub>. At room temperature, a thin film forms on top of partially passivated copper with chlorine present, which is identified to be CuCl by Raman spectroscopy at 77 K. This copper chloride film is locally desorbed by laser heating in vacuum. Deposition-like features are produced on passivated Cu films and CuCl-on-Cu films by laser heating with Cl<sub>2</sub> present. Raman spectroscopy shows that these features are CuCl<sub>2</sub>, with CuCl sometimes also present. After the copper chloride is removed, ~4 μm wide etched features remain in the copper film. The Raman spectrum of anhydrous CuCl<sub>2</sub> presented here is apparently the first such measurement.

## I. INTRODUCTION

The interaction of chlorine with copper films and single crystals has been examined by several investigators to further the understanding of etching in this system. It is currently very difficult to etch this important microelectronics material using dry processing methods, such as plasma chemical etching. At room temperature, chlorine chemisorbs dissociatively on copper.<sup>1,2</sup> Cl diffusion into the Cu, or more likely Cu diffusion through copper chloride to the surface, occurs rapidly at room temperature, especially for Cl<sub>2</sub> pressures exceeding 10<sup>-2</sup> Torr. This leads to the formation of very thick copper chloride films (> 1 μm) on top of Cu structures for suitably high pressures of chlorine (≥ 1 Torr).<sup>3</sup> These CuCl<sub>x</sub> films are produced near the surface with *x* ranging from 0 to 2, corresponding to regions of mixed Cu/CuCl or CuCl/CuCl<sub>2</sub> phases.<sup>3</sup> The etch rates and gas-phase products of copper etching by chlorine have been studied for conventionally<sup>4,5</sup> and excimer laser<sup>6,7</sup> heated copper. For conventional thermal etching, desorbed products are observed for temperatures above ~150 °C.<sup>4</sup> In this study, we examine the transformation and etching of copper films in the presence of chlorine at room temperature and when irradiated by focused laser beams. Whereas, conventional ultrahigh vacuum (UHV) surface probes, such as Auger spectroscopy and x-ray photoemission, were used in many of the above cited studies, Raman spectroscopy is used here for *in situ* analysis.

## II. EXPERIMENTAL METHODS

Copper films (0.1–2 μm thick) were deposited on glass substrates by evaporation and were then mounted in a vacuum reaction chamber, which could be filled with Cl<sub>2</sub> gas. After film evaporation, these samples were handled in three different ways before mounting them in the chamber, which determined the thickness of the copper oxide layer on top of the copper film. They were either stored in vacuum before rapid transfer to the cell (unpassivated copper film), stored under ambient air conditions for several days (several Å copper oxide, partially passivated), or were heated in air for

5–30 min at *T* = 150 °C<sup>7</sup> to form a thick passivation layer [~100–200 Å copper oxide (as Cu<sub>2</sub>O<sup>8</sup>), passivated]. Once placed in the reaction chamber, the sample was viewed with a microscope through a window port in the chamber and was irradiated by a focused cw argon ion laser (4880 Å, ~2.2 μm full width at 1/e intensity, linearly polarized) for local laser heating and for Raman analysis. The unpolarized back-scattered Raman radiation was collected, dispersed by a triple spectrometer, and detected by an intensified diode array. During Raman analysis the sample could be cooled to ~77 K using liquid nitrogen. The chamber was mounted on a translation stage to allow lateral scanning during laser heating. After processing, features were examined by profilometry.

## III. RESULTS

In a series of experiments, unpassivated, partially passivated, and passivated copper films were examined after exposure to Cl<sub>2</sub> at room temperature. These samples were subsequently heated locally by a focused laser either in vacuum or in the presence of Cl<sub>2</sub> and then re-examined. The sequence of typical experiments is portrayed schematically in Fig. 1.

### A. Reactions at room temperature

At ambient temperature, the surface of unpassivated and partially passivated Cu films changed color and developed small cracks after Cl<sub>2</sub> (0.1–20 Torr) was added. After a given exposure, the chlorine was removed and the sample was analyzed *in situ* by Raman spectroscopy. The Raman spectrum of a typical sample (partially passivated) was taken at 298 K after chlorine exposure and is shown in Fig. 2(a). There is a broad featureless peak below 250 cm<sup>-1</sup>. At ~77 K, the Raman spectrum of this sample has three peaks at 145, 170, and 210 cm<sup>-1</sup>, as shown in Fig. 2(b). These three peaks have very nearly the same frequency shifts and relative intensity as the LA + TA, TO, and LO phonon features in the Raman spectrum of crystalline CuCl at 78 K (located at ~151, 175, and 214 cm<sup>-1</sup>, respectively).<sup>9</sup> At ambient tem-

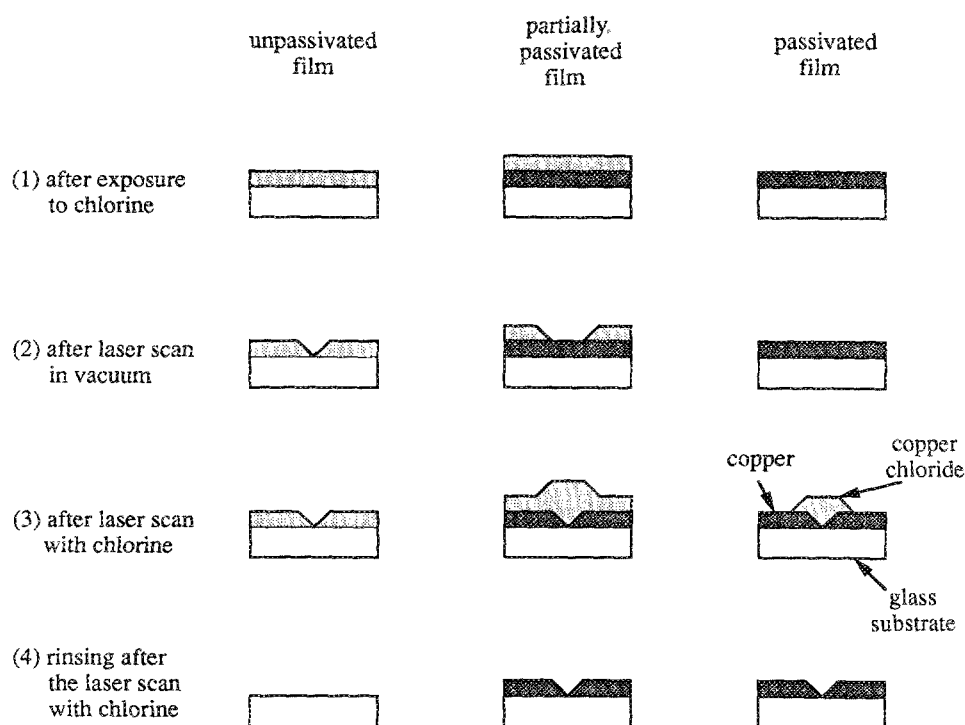


FIG. 1. Schematic representation of experiments conducted here, with the three columns showing different experiments, starting with either an unpassivated, partially passivated or passivated copper film on glass. Throughout the figure, the light shaded area refers to copper chloride, while the dark shaded area represents the copper film. Four stages are shown: (1) after the sample has been exposed to chlorine gas at room temperature, (2) after this exposed sample has been irradiated by a focused laser in vacuum, (3) after the sample has been irradiated by a focused laser with chlorine present, and (4) after rinsing the sample in (3) with a solvent to remove the copper chloride. The processing sequences examined were: (1) alone; (1) followed by (2) [and sometimes followed by rinsing as in (4)]; and (1) followed by (3) and then (4) [with sometimes (3) followed by a laser scan in vacuum as in (2)].

perature, the three CuCl Raman peaks broaden into one nearly featureless peak, as is also seen here for the chlorinated Cu film sample at 298 K [Fig. 2(a)]. The Raman spectrum of partially passivated Cu films subjected to long chlorine exposures at relatively high pressure, e.g., 2 h at 20 Torr, has peaks at 282 and 556  $\text{cm}^{-1}$  in addition to the remaining CuCl peak below 250  $\text{cm}^{-1}$  (298 K).

With thick partially passivated Cu films ( $\geq 1 \mu\text{m}$ ), this

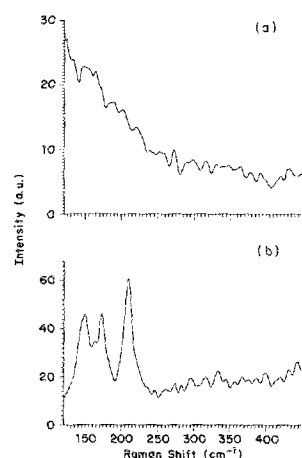


FIG. 2. Raman spectrum of partially passivated copper film ( $1.7 \mu\text{m}$ ) after exposure to 10 Torr  $\text{Cl}_2$  for 10 min with no laser present (Raman analysis with 4880 Å, taken in vacuum): (a)  $T = 298\text{K}$ , and (b)  $T = 77\text{K}$ . These spectra suggest the film is CuCl. The peaks at 145, 170, and 210  $\text{cm}^{-1}$  in (b) are the cuprous chloride LA + TA, TO, and LO phonon features, respectively (Ref. 9).

CuCl film formed on a remaining fraction of the Cu film (Fig. 1). For example, when a  $1.0 \mu\text{m}$  thick Cu film was exposed to 11 Torr  $\text{Cl}_2$  for 120 min, a  $0.6 \mu\text{m}$  thick Cu film remained, which was overlayed by a  $1.6 \mu\text{m}$  thick  $\text{CuCl}_x$  film. After thinner Cu films ( $\sim 1000 \text{Å}$ ) were exposed to chlorine, the film on the glass became yellow and transparent, suggesting that there was no remaining Cu film. Thicker Cu films were totally converted into CuCl only when they were unpassivated. For example, a  $1.0 \mu\text{m}$  thick Cu film was converted to  $4.1 \mu\text{m}$   $\text{CuCl}_x$  with no copper remaining after 15 min of exposure to 12 Torr  $\text{Cl}_2$ , as is expected from Ref. 3. The reaction of Cu with  $\text{Cl}_2$  at room temperature occurred whether or not there was substrate irradiation by ambient room lighting through the window port.

Optical transmission showed that these CuCl films on glass begin to absorb very strongly for  $\lambda < 3800 \text{Å}$ , which is consistent with the 3.2 eV band gap for bulk CuCl with zincblende structure.<sup>10,11</sup> An unfocused 4880 Å laser was directed at near normal incidence onto a  $0.4 \mu\text{m}$  thick copper chloride film on glass to measure the fraction of laser power that was transmitted and reflected. This measurement indicated that about 30% of the incident light was either absorbed or diffusely scattered by the film.

In general, these CuCl films formed by chlorination of partially passivated copper films adhered poorly to the underlying Cu film and could be removed by rubbing or scratching. Alternately, they could be removed by a  $\sim 1.4 \text{M}$  solution of HCl. Measurement of the Cu film thickness before and after chlorine exposure and of the CuCl film thickness, showed that the formation of CuCl and the loss of copper during chlorination could be accounted for by the density change from Cu to  $\text{CuCl}$ .<sup>3</sup>

Exposure of passivated Cu films to chlorine led to no visu-

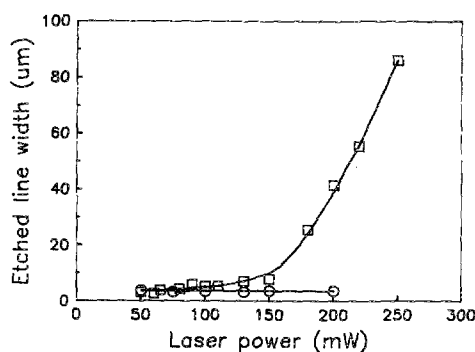


FIG. 3. Width of the etched line measured at the surface after  $\text{CuCl}_x$  ( $2.1 \mu\text{m}$ )-on-Cu ( $0.8 \mu\text{m}$ ) (□) and  $\text{CuCl}_x$  ( $0.4 \mu\text{m}$ ) (○) films on glass were irradiated in vacuum by a scanning ( $5 \mu\text{m/s}$ ) focused  $4880 \text{ \AA}$  laser vs laser power.

al changes in the films ( $10 \text{ Torr Cl}_2$ ,  $4 \text{ h}$ ,  $T = 298 \text{ K}$ ). This was true for films which were oxidized in air at  $150^\circ\text{C}$  for either 5, 20, or 30 min. The Raman spectrum of the surface both before and after exposure to chlorine was unchanged, with peaks at  $149$ ,  $215$ ,  $506$ , and  $646 \text{ cm}^{-1}$  [Fig. 5(a) below], and there was no indication of  $\text{CuCl}$  or  $\text{CuCl}_2$  (see below) after exposure (as depicted in Fig. 1). Crystalline  $\text{Cu}_2\text{O}$  has a strong allowed Raman peak at  $218 \text{ cm}^{-1}$  due to the two-phonon mode  $2\Gamma_{12-}$  ( $4880 \text{ \AA}$ ), and several other weak peaks ( $154$ ,  $515$ ,  $635$ , and  $665 \text{ cm}^{-1}$ ) some of which are forbidden but are observable with resonant excitation.<sup>12</sup> These weak peaks get much stronger after ion-implantation because of the lattice disorder and the resonance with the  $1\text{s}$  exciton. The Raman spectrum obtained here [Fig. 5(a), below] looks very similar to that of damaged crystalline  $\text{Cu}_2\text{O}$ .<sup>12</sup>

## B. Laser irradiation

Laser heating of the  $\text{CuCl}$ -on-Cu films in vacuum locally desorbed part or all of the  $\text{CuCl}$  film, as sketched in Fig. 1. The underlying Cu film always remained intact. These  $\text{CuCl}$ -on-Cu films were made by exposing partially passivated Cu films to  $\text{Cl}_2$ . With substrate scanning during irradiation ( $5 \mu\text{m/s}$  scan speed), the width of the lines etched in the  $\text{CuCl}$  were typically wider than the laser focus ( $\sim 2 \mu\text{m}$  diameter). This width increased rapidly with laser power, as shown in Fig. 3. For  $\text{CuCl}$  films with no underlying Cu film, local laser heating in vacuum also desorbed the  $\text{CuCl}$  locally (Fig. 1), but the etched features were relatively narrow ( $\sim 4 \mu\text{m}$ ) and the widths were independent of laser power (Fig. 3). The Raman spectrum of the  $\text{Cu}_2\text{O}$  passivation layer was examined after laser heating of passivated copper films in vacuum, and was found to be unchanged for laser powers up to  $250 \text{ mW}$ .

In contrast, laser heating of  $\text{CuCl}$ -on-Cu films on glass in the presence of chlorine locally produced a bump, and not the depression expected in etching, as shown in Fig. 1. With scanning, a feature similar to a deposited line was formed, which was wider ( $\sim 30$ – $100 \mu\text{m}$ ) than the laser focus. After subsequent removal of chlorine, a Raman spectrum was tak-

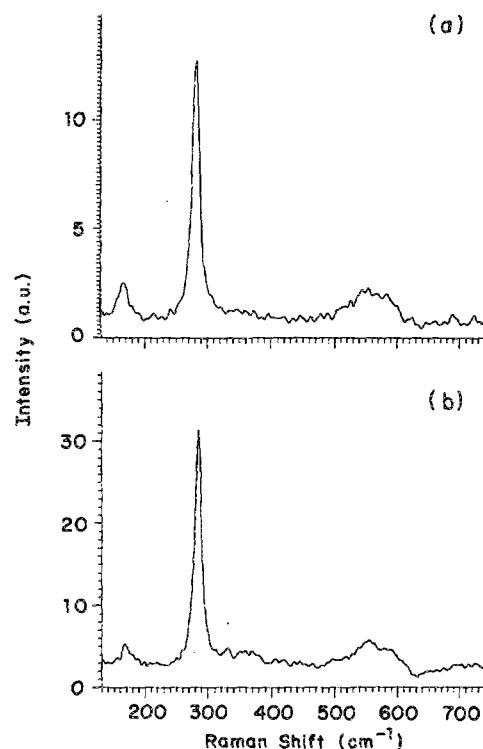


FIG. 4. (a) Raman spectrum taken after laser irradiation of  $\text{CuCl}_x$ -on-Cu film in the presence of chlorine ( $4880 \text{ \AA}$ ,  $20 \text{ mW}$  during scan,  $5 \mu\text{m/s}$  scan rate,  $10 \text{ Torr Cl}_2$ ,  $20 \text{ mW}$  for spectrum). (b) Raman spectrum of  $\text{CuCl}_2$  (anhydrous cupric chloride powder) at room temperature ( $4880 \text{ \AA}$ ,  $20 \text{ mW}$ ).

en of this feature at  $298 \text{ K}$ , giving the spectrum in Fig. 4(a), with a weak peak at  $167 \text{ cm}^{-1}$ , a strong, narrow peak at  $282 \text{ cm}^{-1}$ , and a broad, medium strength peak at  $556 \text{ cm}^{-1}$ . The Raman spectrum of anhydrous  $\text{CuCl}_2$  powder was also measured, giving peaks at  $166$ ,  $283$ , and  $563 \text{ cm}^{-1}$  as shown in Fig. 4(b). This appears to be the first published Raman spectrum of  $\text{CuCl}_2$ . The frequency shifts, widths, and relative strengths of the three  $\text{CuCl}_2$  peaks and those in Fig. 4(a) are very similar, suggesting that the product of local laser heating of  $\text{CuCl}$  films in  $\text{Cl}_2$  is  $\text{CuCl}_2$ . A weak broad peak below  $250 \text{ cm}^{-1}$  is sometimes also seen in these Raman measurements at room temperature, suggesting that there is also some  $\text{CuCl}$  present within the probed depth. A Raman microprobe scan across a typical line ( $80 \text{ mW}$ ,  $5 \mu\text{m/s}$ ,  $13 \text{ Torr Cl}_2$ ) shows that the central portion has a constant  $\text{CuCl}_2/\text{CuCl}$  fraction near the surface, which slowly decreases to zero, and therefore indicating pure  $\text{CuCl}$ ,  $\sim 30 \mu\text{m}$  from the center. This return to pure  $\text{CuCl}$  occurs approximately at the lateral extent of the line ( $\sim 36 \mu\text{m}$ ), as determined by profilometry measurements. On the basis of this identification of  $\text{CuCl}_2$ , the two additional peaks at  $282$  and  $556 \text{ cm}^{-1}$  seen in the room temperature reaction of unpassivated and partially passivated Cu films with very large doses of chlorine are due to  $\text{CuCl}_2$ , suggesting that the film consists of a  $\text{CuCl}/\text{CuCl}_2$  mixed phase under those conditions.

These  $\text{CuCl}_2$  and  $\text{CuCl}$  features were then removed by

dissolving them in 1.4 M HCl, which left the underlying Cu film alone. At the site of the laser heating and localized  $\text{CuCl}_2$  formation, removal of some or all of the Cu film is observed, depending on laser heating conditions (Fig. 1). With scanning, a relatively narrow,  $\sim 4 \mu\text{m}$  wide etched groove is formed in the copper film at low laser power. More generally, the groove widths at the surface ranged from 4–10  $\mu\text{m}$ , tapering down to 0–5  $\mu\text{m}$ , for laser powers ranging from 20–250 mW (5  $\mu\text{m/s}$ , 11.4 Torr  $\text{Cl}_2$ ). After copper chloride removal from  $\text{CuCl}_x$ -on-Cu films, the remaining copper surface had  $\sim 1000 \text{ \AA}$  roughness. Laser heating of the  $\text{CuCl}_2$  bump on  $\text{CuCl}$ -on-Cu/glass in vacuum also desorbed the  $\text{CuCl}_2$  and  $\text{CuCl}$ . At high enough laser intensity, all the copper chloride down to the remaining copper can be desorbed in this manner.

Laser irradiation of  $\text{CuCl}$  films on glass (with no underlying Cu film) in the presence of chlorine locally desorbed the  $\text{CuCl}$  film, producing  $\sim 3\text{--}4 \mu\text{m}$  wide features independent of laser power. Though no bump was observed in this case, which would have indicated the formation of  $\text{CuCl}_2$  (as in the  $\text{CuCl}$ -on-Cu film on glass example), Raman analysis still suggested there was some conversion from  $\text{CuCl}$  to  $\text{CuCl}_2$  near the desorbed region because of the appearance of a strong narrow peak near  $283 \text{ cm}^{-1}$ . Instead of being accompanied by a relatively weak peak at  $563 \text{ cm}^{-1}$ , as in Fig. 4, the  $283 \text{ cm}^{-1}$  peak was accompanied by a comparably strong and broad peak near  $570 \text{ cm}^{-1}$ , which was identified as due to the glass substrate.

Laser heating of passivated copper films in the presence of chlorine produced copper chlorides only with laser powers  $> 40 \text{ mW}$  (1.4  $\mu\text{m}$  thick Cu films). In contrast, continued chlorination of the  $\text{CuCl}_x$ -on-Cu films (partially passivated Cu films) occurred for much lower laser powers,  $\sim 0.5 \text{ mW}$  for the conversion of  $\text{CuCl}$  to  $\text{CuCl}_2$  as probed by Raman spectroscopy and  $\sim 20 \text{ mW}$  for structural changes as probed by profilometry. Real-time Raman analysis during the laser heating scan [5  $\mu\text{m/s}$ , Fig. 5(b)] of passivated copper films showed the  $\sim 280$  and  $560 \text{ cm}^{-1}$  lines of  $\text{CuCl}_2$ , in addition to those of  $\text{Cu}_2\text{O}$  [Fig. 5(a)]. Overlap of the  $\text{Cu}_2\text{O}$  and  $\text{CuCl}$  Raman spectra for shifts below  $250 \text{ cm}^{-1}$ , prevented observation of any  $\text{CuCl}$  in these spectra during the scan. In this real-time probing, the focused 4880  $\text{\AA}$  radiation both locally heated the sample and served as a source of photons for Raman scattering. During these runs the  $\text{Cu}_2\text{O}$  Raman peaks were progressively stronger and the  $\text{CuCl}_2$  peaks were weaker for the Cu films passivated by progressively longer periods of oxidation 5, 20, and 30 min. Raman examination of these features (298 K) after chlorine removal again showed  $\text{CuCl}_2$  and  $\text{Cu}_2\text{O}$ , and also evidence of  $\text{CuCl}$  [Fig. 5(c)]. The  $\text{Cu}_2\text{O}$  peaks in this re-examination were much smaller than those during the chlorination scan because in the latter spectrum the  $\text{Cu}_2\text{O}$  film is still present at the leading edge of scanning laser, while in the former the oxide is no longer present in the center of the probed region and only a weak signal from  $\text{Cu}_2\text{O}$  in peripheral regions is measured.

The copper chloride deposit-line-like features produced on passivated Cu films by laser heating with chlorine present were  $\sim 10\text{--}40 \mu\text{m}$  wide, which is narrower than for the partially passivated Cu films. After removal of copper chloride

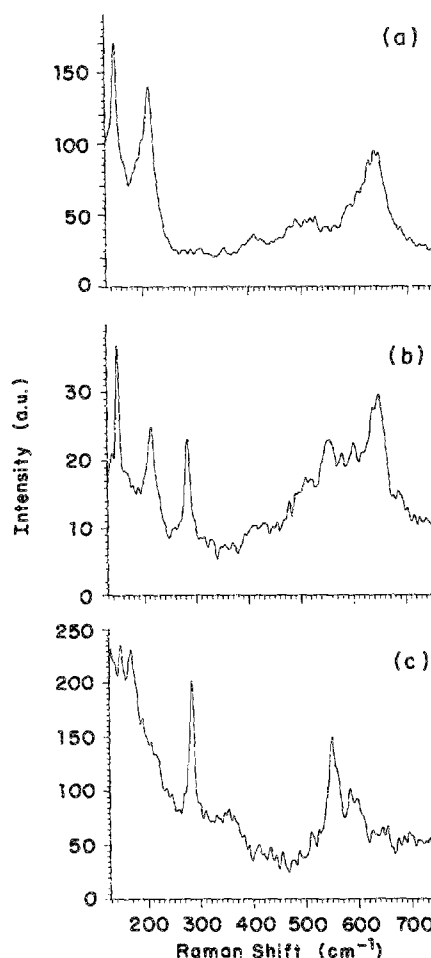


FIG. 5. Raman spectra of passivated copper films using 4880  $\text{\AA}$  (30 min oxidation at  $150^\circ\text{C}$ ): (a) before irradiation (20 mW), (b) in real-time during scan in the presence of 10 Torr  $\text{Cl}_2$  (60 mW, 5  $\mu\text{m/s}$  scan rate), and (c) reanalysis of (b) after scan, in vacuum (20 mW).

by rinsing with hydrochloric acid,  $\sim 4 \mu\text{m}$  wide grooves remained in the copper (independent of laser power). For example, when a 1.38  $\mu\text{m}$  thick Cu film previously oxidized for 30 min at  $150^\circ\text{C}$  was irradiated by 50 mW (5  $\mu\text{m/s}$  scan speed, 10 Torr  $\text{Cl}_2$ ), a Cu groove remained which was 4.4  $\mu\text{m}$  wide at the surface, tapering down to a point 0.44  $\mu\text{m}$  below the surface. The copper chloride feature initially formed during laser heating was 10.8  $\mu\text{m}$  wide at the base, tapering to a width 3.6  $\mu\text{m}$  at a height 1.40  $\mu\text{m}$  above the surface. As sketched in Fig. 1, at the copper surface the copper chloride feature is much broader than the etched copper region for laser heating of both passivated and partially passivated Cu films in chlorine.

Figures 6–8 show the widths and heights of the copper chloride features formed by laser heating of passivated copper films (1.4  $\mu\text{m}$ , 20 min oxidation at  $150^\circ\text{C}$ ) on glass with chlorine [(a), top] and the widths and depths of the copper regions transformed to copper chloride during this process [(b), bottom] for a range of conditions. These stated widths are measured at the surface; in most cases the features became narrower away from the surface.

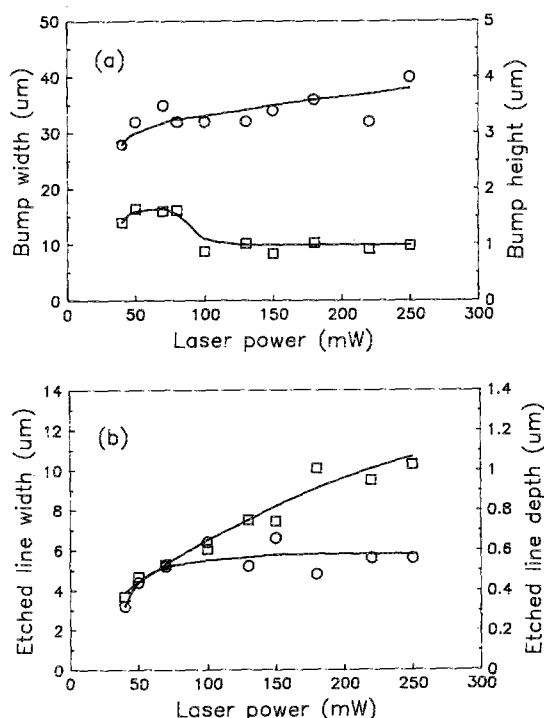


FIG. 6. (a) The width (○) and height (□) of copper chloride features and (b) the width (○) and depth (□) of etched copper features vs laser power after 1.3 μm thick passivated copper films (20 min oxidation at 150 °C) were irradiated with 4880 Å in chlorine. The chlorine pressure is fixed at 10 Torr and the scan rate at 5 μm/s.

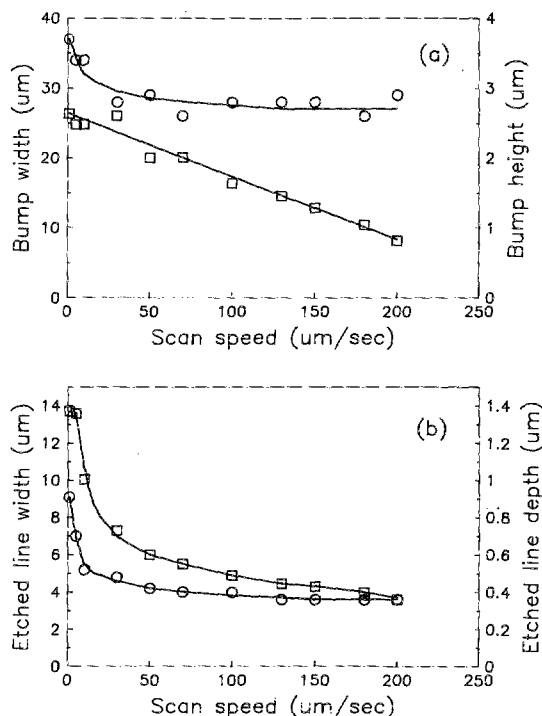


FIG. 8. (a) The width (○) and height (□) of copper chloride features and (b) the width (○) and depth (□) of etched copper features vs scan rate after 1.3 μm thick passivated copper films (20 min oxidation at 150 °C) were irradiated with 4880 Å in chlorine. The laser power is fixed at 50 mW and the chlorine pressure at 50 Torr.

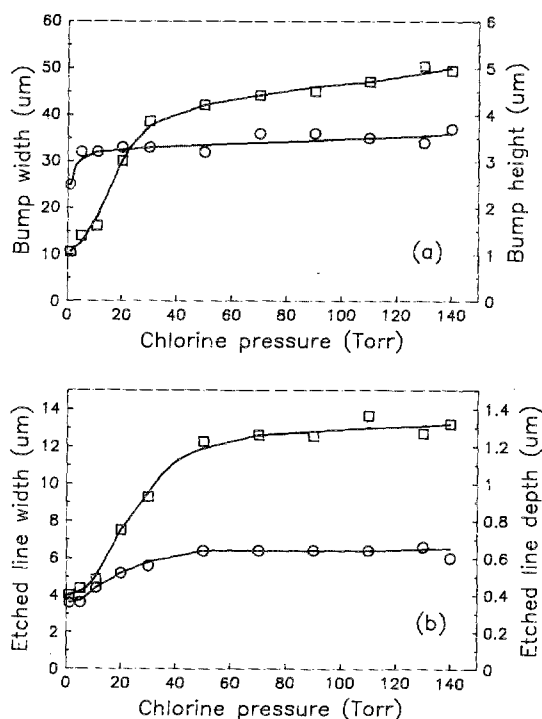


FIG. 7. (a) The width (○) and height (□) of copper chloride features and (b) the width (○) and depth (□) of etched copper features vs chlorine pressure after 1.3 μm thick passivated copper films (20 min oxidation at 150 °C) were irradiated with 4880 Å in chlorine. The laser power is fixed at 80 mW and the scan rate at 5 μm/s.

The laser power was varied in Fig. 6 with the chlorine pressure fixed at 10 Torr and the scan rate at 5 μm/s. With increasing laser power from 50–100 mW, the cross-sectional area of the copper chloride feature decreases, indicating either increased copper chloride density or desorption with increasing laser power. Typically, the depth of the copper etch increased with laser power, with little variation in the width, until the film was totally removed (which is not seen for the example in this figure).

In Fig. 7, the chlorine pressure was varied with the laser power fixed at 80 mW and the scan speed at 5 μm/s. With increasing pressure, the copper chloride feature got taller, while the width remained constant. For pressures above 50 Torr, the 1.4 μm-thick Cu film was almost totally removed and the etch width was fixed at 6 μm.

The scan rate was varied in Fig. 8 with the laser power fixed at 50 mW and the chlorine pressure at 50 Torr. The height of the copper chloride feature and the depth of the copper etch decreased monotonically with scan speed. The etch depth decreased sublinearly with laser dwell time (spot size/scan speed).

In the parameter space spanned by the runs in Figs. 6–8, the top of the copper chloride line formed during laser heating with chlorine present had a concave down profile, which was at times flat on top. However, in some experimental regimes, there was a deep trench down the middle of the line, which was reminiscent of laser heating in vacuum of a previously written copper chloride line. To examine this, an-

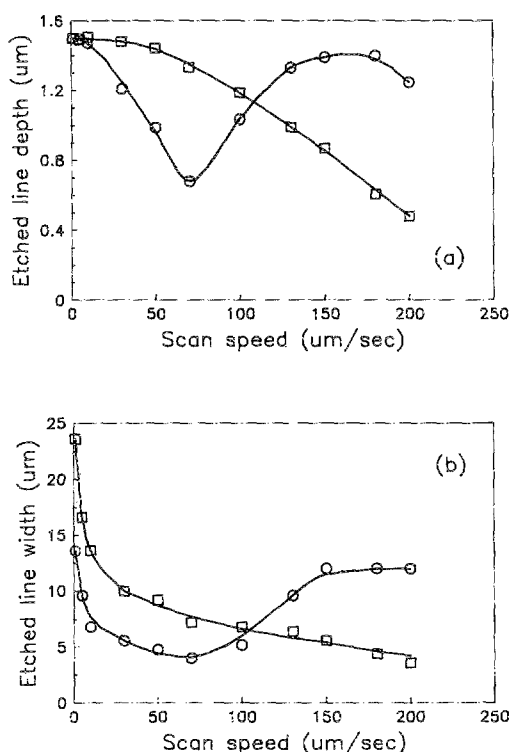


FIG. 9. The (a) depth and (b) width of the etched copper features after copper chloride removal for 400 mW of 4880 Å radiation incident on 1.5 μm thick passivated copper films (15 min oxidation at 150 °C) for chlorine pressures 10 Torr (O) and 120 Torr (□).

other series of experiments was conducted at much higher power, 400 mW, in which the scan rate was varied from 1–200 μm/s (on 1.5 μm thick copper oxidized for 15 min, 10 and 120 Torr Cl<sub>2</sub>). The copper chloride lines formed with deep trenches for the 10 Torr runs only when the scan rate was > 100 μm/s, whereas no trenches or only very shallow trenches were observed for similar runs at 120 Torr. In no case was all the copper chloride removed during the scan.

For these two series of runs, the width and depth of the etched copper region were measured after the copper chloride was removed, and are plotted in Fig. 9. These results look qualitatively like those in Fig. 8 with the etch depth decreasing with increasing scan speed, except for scan rates > 100 μm/s in the 10 Torr Cl<sub>2</sub> run. At these higher scan rates, the etch depth and width begin to increase, until the etch depth almost reaches the thickness of the copper film. There were two small etch side lobes in addition to the main etch pit (whose width is given in Fig. 9). Note that this increase in etch depth for the > 100 μm/s runs correlates with the observation of trenches in the copper chloride lines.

The equivalent vertical etching rate in these experiments is approximately  $(a/b)S$  where  $S$  is the scanning rate,  $a$  is the etch depth, and  $b$  is the etch width. In Figs. 6 and 7 the characteristic vertical etching rate is  $\sim 1$  μm/s with the 5 μm/s scan rate. In Figs. 8 and 9, the fastest vertical etching rate is  $\sim 20$  μm/s for the 200 μm/s scanning rates.

## IV. DISCUSSION

### A. Thin film chemistry

The etching of copper by chlorine entails the transformation of copper to copper chloride (CuCl<sub>x</sub>,  $x = 0-2$ ) and the subsequent desorption of the copper chloride. This first process can be viewed as a sequence of three steps: dissociative chemisorption of chlorine on the copper surface, diffusion of chlorine or copper ions into the bulk, and reaction to form copper chloride. Apparently, each of the experiments performed here involves only one of the two overall steps in etching. The reaction of copper with chlorine at room temperature entails transformation to copper chloride with no desorption. Laser heating of CuCl in vacuum involves desorption only. During laser heating of copper with chlorine present, transformation of copper to copper chloride takes place with little or no apparent desorption of this product in most of the experimental regimes studied here.

With similar copper film thickness and exposure to chlorine at room temperature, the copper chloride films [CuCl<sub>x</sub> ( $x \sim 1$ )] formed in this study with partially passivated Cu films were thinner than those measured by Sesselmann and Chuang for copper films and crystals,<sup>3</sup> but were comparable to those measured in Ref. 3 when the copper films were transferred rapidly to the reaction chamber (unpassivated). This difference is probably due to the formation of a thin copper oxide film during long exposure of the Cu film to air, which may inhibit dissociative chemisorption of Cl<sub>2</sub> or chlorine atom diffusion.<sup>7</sup> For passivated copper films, the thicker Cu<sub>2</sub>O protection film prevents the formation of a copper chloride layer at room temperature in the presence of chlorine. For the unpassivated and partially passivated Cu films, the CuCl<sub>x</sub> ( $x \sim 1$ ) is partially transformed into CuCl<sub>2</sub> for large doses of Cl<sub>2</sub>, or more precisely the spatially averaged value of  $x$  in CuCl<sub>x</sub> increases for large chlorine exposures.<sup>3</sup> No complete etching cycle is expected in these experiments at room temperature, because desorption of copper chloride occurs only for  $T > 150$  °C.<sup>4</sup>

If the CuCl<sub>x</sub>-on-Cu film formed when a partially passivated copper film is exposed to chlorine is irradiated by a focused laser in vacuum, the underlying Cu film is heated by the laser and the CuCl<sub>x</sub> ( $x \sim 1$ ) layer on top is thermally desorbed. If chlorine is present during irradiation, there is local chlorination of the CuCl<sub>x</sub> ( $x \sim 1$ ) film to CuCl<sub>y</sub> ( $y \sim 2$ ) and of the underlying Cu film to CuCl<sub>z</sub>. Because the molecular volumes for CuCl<sub>y</sub> and CuCl<sub>z</sub> increase as  $y$  and  $z$  increase, a bump is expected to form if the copper chloride does not also desorb. Desorption of these local copper chloride features, which is the second part of etching, is also expected to occur at elevated temperatures. However, in most of the regimes studied here, it appears that there is only noticeable further growth of CuCl<sub>2</sub> when chlorine is present. With no chlorine present, these CuCl<sub>2</sub> bumps can be desorbed by laser heating.

With initially passivated films, the Cu is locally transformed to CuCl/CuCl<sub>2</sub> mixed phases by laser heating, also with no apparent sign of desorption in most cases. Copper chloride lines formed with a deep depression in the center were observed in some experimental regimes, suggesting



limited desorption of the copper chloride. With an overlaying copper oxide film, there is no reaction with chlorine to form  $\text{CuCl}_x$  at room temperature and the laser power needed to begin this reaction must exceed a threshold value. Because of this threshold, the copper chloride and etched copper regions that are formed during laser heating of passivated copper with chlorine present are narrower than those formed during processing of partially passivated copper. Laser heating of the passivated film does not remove the  $\text{Cu}_2\text{O}$  layer; added chlorine gas is necessary.

The ratio of the number of copper atoms that are transformed to copper chloride and remain on the surface to the total number of Cu atoms that are transformed to copper chloride during scanned laser heating of copper with chlorine present was determined from the cross-sectional areas of the copper chloride and etched copper regions and the known densities of Cu and either  $\text{CuCl}$  or  $\text{CuCl}_2$ . If this ratio were found to be less than unity, it would indicate copper chloride desorption as well as formation during laser heating of copper films with chlorine present. Instead, the ratio was found to be  $\sim 2\text{--}4$  for lines without trenches, suggesting that the copper chloride features are porous, with lower than bulk density. No conclusions can be drawn about possible desorption.

Though it is not obvious from previous studies<sup>1-7</sup> whether dissociative chemisorption of chlorine, Cl or Cu migration into the bulk, Cu/Cl reactions, or copper chloride desorption would be the rate limiting step in laser assisted etching of copper by  $\text{Cl}_2$ , desorption clearly appears to be a limiting step here. A typical rate of desorbing copper chlorides in vacuum in these laser heating experiments is  $\sim 5\text{ }\mu\text{m/s}$ . This is also a characteristic rate of copper chloride formation during laser heating of copper in the presence of chlorine. Using known equilibrium sublimation pressures, the evaporation rate of  $\text{CuCl}$  is  $\sim 5\text{ }\mu\text{m/s}$  (expressed as a film etching rate) at  $\sim 650\text{ K}$ , while  $\text{CuCl}_2$  has this same evaporation rate at  $\sim 700\text{ K}$ .<sup>13</sup>  $\text{CuCl}_2$  can also decompose into  $\text{CuCl}$  and chlorine, though this becomes important only above  $900\text{ K}$  in the absence of high chlorine pressures.<sup>13</sup> These estimates must be taken with caution since the products and processes involved in thermal desorption of these chlorinated copper films can be very different from those of  $\text{CuCl}$  or  $\text{CuCl}_2$ .<sup>6</sup> Still, using the evaporation rate of  $\text{Cu}_3\text{Cl}_3$  from chlorinated Cu (100) (presumably  $\text{CuCl}_x$ ,  $x \sim 1$ ),<sup>4</sup> measured by temperature programmed desorption (and extrapolated to slightly higher temperatures here), a  $\sim 5\text{ }\mu\text{m/s}$  etch rate of chlorinated copper is expected at  $\sim 600\text{ K}$ . This is close to the  $650\text{ K}$  estimate for  $\text{CuCl}$  given above. Therefore, it is estimated that laser etching of the copper chlorides requires  $T \sim 600\text{--}700\text{ K}$  locally, or a temperature rise of  $\sim 300\text{--}400\text{ K}$ , to obtain the needed desorption rates. The desorption rate increases by a factor of 2 with each additional  $\sim 15\text{ K}$  temperature rise.

In most of the experiments conducted here, the local laser heating of the evaporated copper film is the most important effect of the focused beam. The copper film is a good thermal conductor (thermal conductivity  $3.98\text{ W/cm K}$  for bulk copper),<sup>11</sup> while the glass substrate is a poor thermal conductor ( $14\text{ mW/cm K}$ )<sup>11</sup> as is any overlaying copper chlo-

ride film (which should have a thermal conductivity less than that of bulk  $\text{CuCl}$ ,  $8.4\text{ mW/cm K}$ ).<sup>11</sup> The steady-state surface temperature rise during laser heating was calculated, as outlined in the Appendix, for two model cases of relevance. One case examined was that of a copper film on a glass substrate, where all nonreflected light is absorbed by the copper, which simulates laser heating of passivated copper in the presence of chlorine. This is only a crude approximation to the actual conditions because a local copper chloride overlayer forms in the laser irradiated region during scanning. The measured reflectivity of the copper films at  $4880\text{ Å}$  was used in the calculation,  $\sim 40\%$  for passivated films, which is less than the published value for freshly evaporated films at this wavelength,  $61\%$ .<sup>14</sup> The second case was a copper chloride film on glass, which simulates several laser heating and desorption experiments conducted here. The upper limit of the absorption coefficient of these copper chloride films measured here at  $4880\text{ Å}$  was used ( $1/\mu\text{m}$ ), along with the measured reflectivity,  $10\%$ . All parameters were assumed to be independent of temperature, which is a good approximation in both cases examined, so the calculated temperature rise scales linearly with laser power, with the beam radius fixed at the measured value ( $1.1\text{ }\mu\text{m}$ ). Heat flow into the gas is neglected in the calculations.<sup>15</sup>

As seen in Fig. 10, the temperature profile in the Cu-on-glass case is much broader than for copper chloride-on-glass, and for that matter much broader than for a semi-infinite copper substrate, because thermal diffusion is essentially two-dimensional for Cu-on-glass and is three-dimensional in these other cases. Fig. 11 shows the temperature rise at the center of the laser spot, which scales linearly with laser power, for these two cases.

Figure 10(b) suggests that a laser with power of  $50\text{ mW}$  incident on  $\text{CuCl}$  ( $0.4\text{ }\mu\text{m}$ )-on-glass (as in Fig. 3) will increase the surface temperature by an estimated  $2750\text{ K}$  at the center of the laser spot and  $\sim 930\text{ K}$  a distance  $2\text{ }\mu\text{m}$  away. Though there is great uncertainty in the absorption coefficient, which is probably  $< 1/\mu\text{m}$ , making these estimated temperature rises too high, this still suggests that the laser powers used in Fig. 3 are high enough to desorb  $\text{CuCl}_x$  from  $\text{CuCl}$ -on-glass. The desorbed features are narrow because the temperature profile in Fig. 10(b) is narrow and because laser absorption and the temperature rise both decrease as  $\text{CuCl}$  is etched from the center.

Figure 11(a) indicates that much higher laser powers must be used to reach this same temperature rise for Cu-on-glass. With  $200\text{ mW}$  incident there will be a  $\sim 200\text{ K}$  rise in temperature for a  $1.0\text{ }\mu\text{m}$  thick film and  $\sim 160\text{ K}$  for a  $1.3\text{ }\mu\text{m}$  thick film. Since the thermal conductivity of the evaporated film is probably less than the bulk value used here, the temperature rises in Figs. 10(a) and 11(a) are probably somewhat underestimated. Still, this suggests why in Figs. 6-8 there was no sign of copper chloride desorption. The measured rate of forming  $\text{CuCl}_x$  during a scan was  $\sim 1\text{--}20\text{ }\mu\text{m/s}$ , but the temperature rise was too small for the desorption rate to be competitive. (As discussed earlier, once the scan has started and  $\text{CuCl}_x$  has formed on top of the Cu-on-glass, as in Figs. 6-8, the temperature rise at the surface will probably be smaller than these estimates during steady state



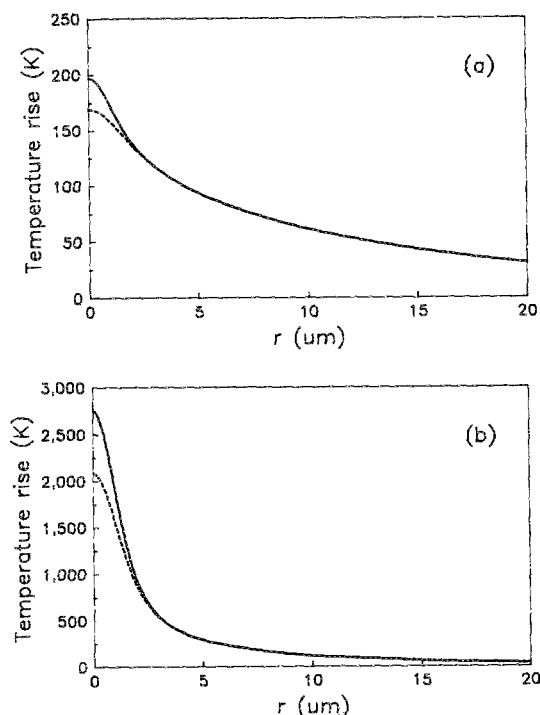


FIG. 10. Calculated temperature rise due to laser heating vs radial distance  $r$  for (a)  $1.0\text{ }\mu\text{m}$  thick Cu-on-glass (200 mW incident) and (b)  $0.4\text{ }\mu\text{m}$  thick  $\text{CuCl}_2$ -on-glass (50 mW incident). The solid line is the temperature rise at the top of the film (film/gas interface) and the dashed line is the rise at the bottom of the film (film/glass interface). See the appendix for details of the calculation.

scanning.) For the runs shown in Fig. 9 (400 mW,  $1.5\text{ }\mu\text{m}$  Cu films), the estimated temperature rise is  $\sim 290\text{ K}$ , which is closer to that needed for competitive desorption.

If the rate of  $\text{CuCl}_x$  desorption from the surface exceeded that of  $\text{CuCl}_x$  formation, clean copper grooves with the characteristic  $\sim 4\text{ }\mu\text{m}$  width would be produced. If the  $\text{CuCl}_x$  desorption rate were slower than that for  $\text{CuCl}_x$  formation, copper chlorides would remain on the surface. This latter case apparently describes the experiments reported in Figs. 6–8. Since conversion from Cu to  $\text{CuCl}_x$  entails a 310% volume increase, the copper chloride expands forming a deposit-like feature that is much wider than is the copper etch and is much taller than the copper etch is deep. The copper chloride line may be porous because of this rapid and large expansion. Since the lateral dimensions of the  $\text{CuCl}_x$  features are much wider than the laser spot size, the leading edge of the copper chloride line precedes the laser focus during the scan. Consequently, in steady state the laser is incident on a thick  $\text{CuCl}_x$  feature atop Cu, even when the Cu has been passivated. With the weak absorption by the  $\text{CuCl}_x$  and its small thermal conductivity, the  $\text{CuCl}_x$ -Cu interface (where continued copper chlorination occurs) is hot because it is near the site of laser heating of the copper, while the  $\text{CuCl}_x$ /gas interface may be too cold for  $\text{CuCl}_x$  desorption. The trenches in the  $\text{CuCl}_x$  features and the rapid transformation of Cu to  $\text{CuCl}_x$  seen for fast scan speeds (400 mW,  $> 100\text{ }\mu\text{m/s}$ , 10 Torr  $\text{Cl}_2$ ) may indicate conditions where desorption is competitive with copper chloride formation. At lower laser powers, the surface temperatures are not

high enough to promote desorption. At slower scan speeds and for higher pressures, the leading edge of the reaction may precede the laser, leading to a cooler surface.

Visible light photolysis of gas-phase  $\text{Cl}_2$  to form free chlorine atoms<sup>16</sup> could affect these observations. The chlorination of copper films at room temperature was found to be the same with or without ambient room light impinging on the sample, so this potential source of Cl atoms is not important. It is difficult to assess the importance of free Cl atoms formed near the substrate by  $4880\text{ }\text{\AA}$  photolysis of  $\text{Cl}_2$  during the laser heating experiments.

Raman analysis has been used here to identify non-desorbed  $\text{CuCl}$  and  $\text{CuCl}_2$ . It is not capable of measuring the Cu/CuCl ratio in a  $\text{CuCl}_x$ ,  $0 < x < 1$  mixed phase because Raman methods are insensitive to Cu. The absolute ratio of  $\text{CuCl}/\text{CuCl}_2$  in a uniform  $\text{CuCl}_x$ ,  $1 < x < 2$  mixed phase can be determined by using Raman spectroscopy and calibration by other thin film probes,<sup>3</sup> since both  $\text{CuCl}$  and  $\text{CuCl}_2$  have strong Raman spectra. However, since the  $\text{CuCl}/\text{CuCl}_2$  ratio probably varies with depth in the samples of this study and the Raman probed depth also varies with this ratio, calibration was not attempted here. [Since  $\text{CuCl}$  is fairly transparent to the  $4880\text{ }\text{\AA}$  laser, the Raman spectrum probes the entire film thickness ( $x = 1$ ). For mixed  $\text{CuCl}/\text{CuCl}_2$  phases, the probe depth is less certain.] Therefore, only the relative  $\text{CuCl}/\text{CuCl}_2$  ratios (from the uncalibrated Raman peak strengths) were determined here and used to examine variations in relative  $\text{CuCl}$  and  $\text{CuCl}_2$  content across the surface.

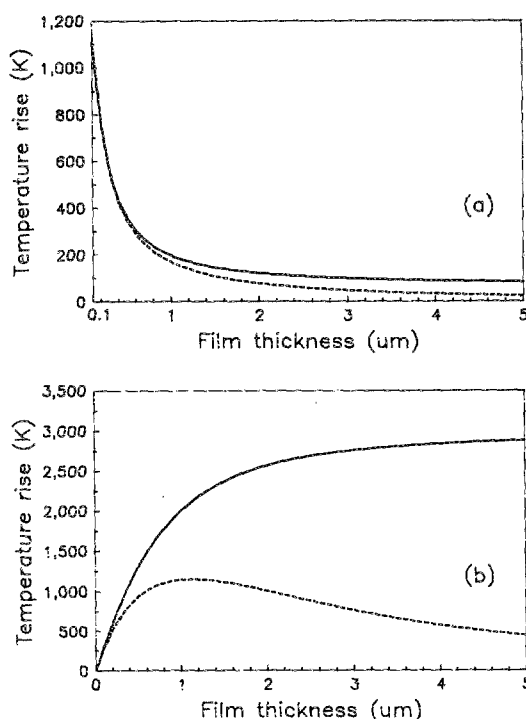


FIG. 11. The temperature at  $r = 0$  at the top of the film (solid line) and bottom of the film (dashed line) as a function of film thickness for (a) Cu-on-glass (200 mW) and (b)  $\text{CuCl}_2$ -on-glass (20 mW). The laser-induced temperature rises in this figure and Fig. 10 vary linearly with the incident laser power. See the appendix for further details.

## B. Patterning implications

Local laser patterning of Cu films without total passivation unavoidably entails loss of at least part of the Cu film to the formation of  $\text{CuCl}_x$  by thermal reactions with chlorine at room temperature. With no passivation, an entire  $\sim 1 \mu\text{m}$  thick Cu film can convert rapidly to copper chloride with several Torr chlorine pressure. With partial passivation, a relatively controllable thickness of copper chloride forms, leaving an underlying Cu film. If the copper film is totally passivated, as with a  $\sim 100\text{--}200 \text{ \AA}$  thick copper oxide overlayer, no significant copper chloride will form.

Two modes of patterning of copper films on transparent insulators are possible, alternately involving local formation or desorption of copper chloride:

(1) Direct patterning can occur by local heating of passivated copper films with chlorine present to produce local regions of copper chloride. Partially passivated copper films could also be used. In either instance, all copper chloride features can be removed afterwards by thermal desorption in vacuum or by using a conventional large area etch that selectively etches copper chloride vis-a-vis copper, e.g., hydrochloric acid. Spatial resolution with this method is  $\sim 4 \mu\text{m}$  in either case, which approaches the laser spot size. However, use of the passivated copper film is preferred because no copper is lost to copper chloride formation, and because after copper chloride removal the remaining Cu film is smooth with the first method using passivated copper films but is  $\sim 1000 \text{ \AA}$  rough with the second method using partially passivated films.

(2) An alternate approach involves patterning the  $\text{CuCl}_x$  film overlaying a Cu film, by local desorption using laser heating in vacuum. The overlaying  $\text{CuCl}_x$  film could be formed by chlorination of either a partially passivated Cu film or an unpassivated copper film that has been deposited on a previously passivated Cu film; the latter approach is preferred. The patterned  $\text{CuCl}_x$  serves as a mask for a second step in which the exposed regions of the underlying Cu film are selectively etched vis-a-vis the  $\text{CuCl}_x$  using a conventional large area etching process.

The first mode of patterning is preferred because it involves fewer steps and may lead to finer spatial resolution. Copper etching with no residual copper chloride may occur under certain experimental conditions where desorption is faster than copper chloride formation (high power, low  $\text{Cl}_2$  pressure, fast scan rates). However, if etching with very little concomitant temperature rise is required, e.g., for Cu films on polyimide, operating with low laser power may be preferred. The copper chloride would not be desorbed during the laser scan but instead would be removed afterwards.

## V. CONCLUDING REMARKS

Laser-assisted thermal reactions of copper films in the presence of chlorine transform copper locally to  $\text{CuCl}$  and  $\text{CuCl}_2$ . Under some experimental conditions there is evidence for copper chloride desorption during laser heating.

Further study of the regimes where product desorption is complete is of interest. *In situ* Raman spectroscopy of  $\text{CuCl}$ ,  $\text{CuCl}_2$ , and  $\text{Cu}_2\text{O}$  films has been shown to be a valuable probe of the progress of these thin film reactions.

## ACKNOWLEDGMENTS

The authors would like to acknowledge support by the Office of Naval Research and IBM, and the assistance of J. A. Tuchman in the temperature calculation and P. Shaw in the copper chloride absorption measurements.

## APPENDIX

The approach used by Lax<sup>17</sup> to calculate the temperature rise during steady state laser heating of a semi-infinite substrate was extended here to the case of an absorbing film on a transparent semi-infinite substrate.

Consider a film of thickness  $L$  ( $z = 0\text{--}L$ ) with absorption coefficient  $\alpha$  and thermal conductivity  $K_1$  on a semi-infinite transparent material with thermal conductivity  $K_2$  ( $z \geq L$ ). It is irradiated by a laser of power  $P$  with a Gaussian intensity profile with half-width at  $1/e$  intensity points of  $w$ . The film has reflectivity  $R_{\text{refl}}$ . The temperature rise in the film  $T_1(r, z)$  is the sum of the specific solution of the steady state heat flow equation<sup>17</sup>:

$$T_{1,\text{spec}} = -B \exp(-WZ) \int_0^\infty \frac{J_0(\lambda R) F(\lambda) \lambda}{W^2 - \lambda^2} d\lambda \quad (\text{A1})$$

and the homogeneous solution:

$$T_{1,\text{homog}} = \int_0^\infty [G(\lambda) \exp(-\lambda Z) + H(\lambda) \exp(\lambda Z)] \times \frac{J_0(\lambda R) F(\lambda) \lambda}{W^2 - \lambda^2} d\lambda \quad (\text{A2})$$

while in the semi-infinite medium the temperature rise is due to the homogeneous solution:

$$T_{2,\text{homog}} = \int_0^\infty Q(\lambda) \exp(-\lambda Z) \frac{J_0(\lambda R) F(\lambda) \lambda}{W^2 - \lambda^2} d\lambda. \quad (\text{A3})$$

The normalized coordinates  $R = r/w$ ,  $Z = z/w$ , and  $W = \alpha w$  have been used. Also,

$$F(\lambda) = \frac{1}{2} \exp(-\frac{1}{4} \lambda^2) \quad (\text{A4})$$

and

$$B = \alpha P (1 - R_{\text{refl}}) / \pi K_1. \quad (\text{A5})$$

After matching the boundary conditions of no heat flow at  $z = 0$ <sup>15</sup> and continuity of temperature and heat flow at  $z = L$ , the general solution for the temperature rise everywhere is obtained. For simplicity, only the expression for the temperature rise at the top of the film that was used to obtain Figs. 10 and 11 is given here:

$$T_1(R, Z = 0) = B \int_0^\infty M(\lambda) \frac{J_0(\lambda R) F(\lambda)}{W^2 - \lambda^2} d\lambda \quad (\text{A6})$$

where

$$M(\lambda) = \frac{[K_1 + K_2](\lambda - W) \exp(\lambda L) - [K_1 - K_2](\lambda + W) \exp(-\lambda L) + 2[W K_1 - \lambda K_2] \exp(-\lambda L)}{[K_1 - K_2] \exp(-\lambda L) - [K_1 + K_2] \exp(\lambda L)}. \quad (\text{A7})$$

The thermal conductivities given in the text were used, along with the measured spot size,  $w = 1.1 \mu\text{m}$ . An absorption coefficient of  $1/\mu\text{m}$  was used for CuCl, which is an upper limit estimate derived from experiments. Though reflection at the gas/CuCl interface was included, reflection at the CuCl/glass interface was neglected; the measured reflection coefficient, 10%, was used in the calculation. The laser was totally absorbed by the Cu in the Cu/glass example. The results of these calculations are plotted in Figs. 10 and 11.

<sup>1</sup>P. J. Goddard and R. M. Lambert, *Surf. Sci.* **67**, 180 (1977).

<sup>2</sup>D. Westphal and A. Goldmann, *Surf. Sci.* **131**, 92, 113 (1983).

<sup>3</sup>W. Sesselmann and T. J. Chuang, *Surf. Sci.* **176**, 32, 67 (1986).

<sup>4</sup>H. F. Winters, *J. Vac. Sci. Technol. B* **3**, 9 (1985); H. F. Winters, *J. Vac. Sci. Technol. A* **3**, 786 (1985).

<sup>5</sup>S. Park, T. N. Rhodin, and L. C. Rathburn, *J. Vac. Sci. Technol. A* **4**, 168 (1986).

<sup>6</sup>W. Sesselmann, E. E. Marinero, and T. J. Chuang, *Surf. Sci.* **178**, 787 (1986); *Appl. Phys. A* **41**, 209 (1986).

<sup>7</sup>J. J. Ritsko, F. Ho, and J. Hurst, *Appl. Phys. Lett.* **53**, 78 (1988).

<sup>8</sup>R. J. Nika and P. M. Hall, *IEEE Transactions, Components, Hybrids and Manufacturing CHMT-2*, 412 (1979).

<sup>9</sup>T. Fukumoto, S. Nakashima, K. Tabuchi, and A. Mitsuishi, *Phys. Status Solidi B* **73**, 341 (1976).

<sup>10</sup>For example, see *Optical Properties of Solids*, edited by S. Nudelman and S. S. Mitra (Plenum, New York, 1969); *Thermal Radiative Properties: Nonmetallic Solids*, edited by Y. S. Touloukian and D. P. DeWitt (Plenum, New York, 1972).

<sup>11</sup>*CRC Handbook of Chemistry and Physics*, 69th ed., edited by R. C. Weast (Chemical Rubber, Boca Raton, FL, 1988–1989).

<sup>12</sup>D. Powell, A. Compaan, J. R. Macdonald, and R. A. Forman, *Phys. Rev. B* **12**, 20 (1975).

<sup>13</sup>*Halides of the First Row Transition Metals*, by R. Colton and J. H. Canterford (Wiley-Interscience, London, 1969).

<sup>14</sup>*American Institute of Physics Handbook*, edited by D. E. Gray, 3rd ed. (McGraw-Hill, New York, 1972) pp. 6–133.

<sup>15</sup>Cooling by conduction to the  $\text{Cl}_2$  gas should decrease these temperature rises by  $< 0.1\%$  for Cu-on-glass and by  $\sim 10\%$  for CuCl-on-glass. Convection could decrease these laser-assisted temperature increases even more. H. Tang and I. P. Herman, (unpublished).

<sup>16</sup>M. A. A. Clyne and J. A. Coxon, *J. Mol. Spectrosc.* **33**, 381 (1970); H. Okabe, *Photochemistry of Small Molecules* (Wiley-Interscience, New York, 1978).

<sup>17</sup>M. Lax, *J. Appl. Phys.* **48**, 3919 (1977).